Electronic Journal of Structural Engineering

Original Article

Cite this: DOI:10.56748/ejse.25774

Received Date: 4 March 2024
Accepted Date: 10 July 2025

1443-9255
https://ejsei.com/ejse


# Bridge Structural Damage Identification Technique Based on BPNN and Vehicle-bridge Interaction Analysis

**Lingling Li [a*], Yibo Zhang [a]**
[a] School of Civil Engineering and Transportation Engineering, Yellow River Conservancy Technical University, Kaifeng 475000, China
*Corresponding author: baolingli1216@163.com

## Abstract

The traditional method of detecting bridge conditions cannot continuously monitor and maintain bridges during use. To address this issue, the study proposed a damage identification method that uses a back-propagation neural network and vehicle-bridge coupling. The method analyzed the car's response when passing over the bridge using a back-propagation neural network combined with the coupled vibration of the vehicle-bridge. It then inferred the response of the car tire's contact point with the bridge. To create a model of the simulated bridge's damaged structural response, the stiffness of the bridge contact point was decreased. The contact point between the bridge deck and the tires was used as input for a back-propagation neural network that computed coupled vibration equations for the vehicle and the bridge and created a data set of their responses. The network can also accurately locate damaged bridge structures and assess the extent of the damage. The results demonstrated that the average accuracy of the back-propagation neural network in locating the damaged bridge structure was about 90%. Under circumstances where varying noise levels were present, the average accuracy in locating the damaged structure was kept at 85%. The maximum accuracy in assessing the degree of damage to the structure was 98.54%, around 10% higher than the performance of deep belief networks and support vector machines in identifying damage to bridge structures. Taken together, the proposed method for identifying damage to bridge structures can achieve high localization and quantitative accuracy.

## Keywords

**Back-propagation neural network, Vehicle-bridge coupling, Bridge structure, Damage identification, Axle displacement response**

## 1. Introduction

Numerous regional routes feature bridges, which play a crucial role in transportation for military and security purposes, as well as economic mobility (Yessoufou & Zhu, 2023). Although long-term bridge use does not immediately pose a major safety issue, it can seriously compromise the bridge's structural stability over time, potentially causing it to collapse. Wind, rain, and passing vehicles can affect the structure of the bridge to varying degrees (Malekjafarian et al., 2019). For instance, the Zhashui Bridge in Shaanxi Province collapsed on July 19, 2024, due to unexpected intense rainfall and flash flooding. Similarly, on October 10, 2019, the Xigang Road Bridge in Jiangsu Province collapsed due to an overload of cars colliding with the bridge (Nguyen et al., 2019; Sony et al., 2022). Each instance of bridge collapse resulted in financial losses and human casualties, significantly affecting the long-term stability of society. Therefore, identifying and maintaining the structure of the bridge is crucial because several factors can cause it to collapse. These factors include the bridge's lengthy working hours, which can damage its internal structure, cars passing through it, the force of the cars' tires on the bridge, the vibration the cars cause on the bridge, and other factors (Neves et al., 2021). During use, the structure of a bridge not only bears the effect of vehicle loads, but also the impact force generated by the contact between the car and the bridge when the vehicle is traveling across the bridge. Most of the bridges cross large rivers, resulting in unsustainable and more difficult inspection and maintenance (Hao et al., 2020; Zong & Yi, 2020). The traditional bridge inspection method has poor identification and localization accuracy for damaged structures, as well as poor accuracy in identifying the degree of structural damage. Therefore, this study uses a combination of a back-propagation neural network (BPNN) and vehicle-bridge coupling to identify damage to bridge structures, with the expectation that it would improve the accuracy of identifying structural damage to bridges and promote the development of the field of bridge damage. This study innovates by combining BPNN and vehicle-bridge coupling vibration analysis. This combination simultaneously utilizes BPNN's mapping ability for complex relationships and vehicle-bridge coupling vibration analysis's ability to capture dynamic responses. This provides a new perspective and method for identifying bridge damage.
The main contribution of this study is as follows:

1) It is an efficient and accurate technical means of identifying damage to bridge structures. It can quickly process large amounts of bridge vibration response data and effectively identify damage characteristics.
2) The proposed method for assessing bridge structure damage can be adapted to different types of bridges and damage modes. It is scalable, providing a universal solution for identifying damage to different types of bridges.

### 1.1 Related Work

In recent years, with the gradual increase in the number of bridges, it has received extensive attention from scholars at home and abroad as to how to continuously carry out bridge inspection and maintenance and improve the identification accuracy of structural damage of bridges. To solve the problem of low bridge damage identification accuracy, Wu et al. proposed a bridge damage identification method based on BP neural network. The study utilized bridge vibration to improve recognition accuracy and established a bridge finite element model. The neural network was also validated using random samples. The results indicated that the mean square error was 0.003196 and the correlation coefficient r=0.9654, which could effectively detect the bridge state (Wu & Zhang, 2023). He et al. proposed a neural network with a depth structure to address the limited ability of traditional recognition methods to detect subtle bridge damage. To develop a damage recognition method based on a convolutional neural network and recurrence maps, the coupling between vehicles and bridges was analyzed using wavelet packet filtering and reconstruction. The resulting recurrence maps were then used as input images for the neural network (He et al., 2021). To detect and evaluate deterioration in bridges' structural integrity, Chen and his colleagues developed a two-dimensional convolutional neural network identification technique based on continuous wavelet variation. They combined the vehicle-bridge coupling model with a deep learning model to simulate bridge damage by reducing the stiffness of the unit. Then, they used the vehicle-bridge coupling vibration to obtain the response signal and construct a data set to identify the damage (Chen et al., 2024). In response to the problems of large workloads, long time consumption, and the inability to quickly predict the finite element model, Li et al. proposed a BPNN-based stress and displacement prediction model for bridge structures. They created a three-dimensional rod system finite element model and an artificial neural network bridge structural response model and enhanced the training and test data sets for the finite element models (Zhao, 2024). The members of Nick et al. addressed the issue that vibration-based damage identification methods were unreliable in the presence of noise. They proposed a method to quantify the degree of damage using artificial neural networks. The study utilized modal flexibility damage indices with different damage levels as inputs for neural

network training and used the modal flexibility method to eliminate noise and locate damage (Nick & Aziminejad, 2021).

Furthermore, academics both domestically and internationally are highly concerned about vehicle-bridge coupling. Zhang et al. proposed a damage identification method based on macroscopic strain patterns for bridges with large stiffness, strong time-varying vibration characteristics, and smooth vehicle loads. These characteristics made it difficult to determine the strain patterns of bridges. They utilized wavelet transform denoising and reconstruction techniques to reconstruct the static and dynamic strain data of vehicle-bridge coupling. They combined the mutual correlation function to construct a matrix damage localization index (Zhang et al., 2022). To address the limitations of current techniques for identifying bridge damage in vehicle-bridge coupling systems, Chen et al. proposed an approach integrating the coupled vibration responses of vehicles and bridges with a deep learning model. First, they established a model of the vehicle and bridge, used unit stiffness to simulate bridge damage, and carried out a coupled vehicle-bridge vibration analysis under different flatness conditions (Chen et al., 2024). To detect damage to bridges with identical cross sections, (Zhi et al., 2023). proposed a method based on the coupled vibration of vehicles and bridges. First, they determined the bridge's vibration mode function. Then, they simulated a car traveling over it and solved the coupled equations. Finally, they analyzed the car's and bridge's reactions at the damaged site. Additionally, this method does not require special signal processing. Corbally et al. addressed the inability of bridges to be consistently inspected and the maintenance of infrastructure by proposing a method to monitor bridge conditions using wheel response to bridge contact points. The study measured the axle contact point response from within the vehicle to infer the sensitivity of the axle contact point response to the roadway. A rigid disk was also used to simulate axle interactions (Corbally & Malekjafarian, 2021).

Research conducted both domestically and abroad has revealed drawbacks to the traditional approach to detecting damaged bridge structures, including an inability to track the bridge's condition over time and low accuracy in locating and identifying damage. The project is proposed to identify damaged bridge structures by combining a BPNN with a vehicle-bridge coupling. This method is expected to enable continuous monitoring of bridge status while improving the accuracy of identifying structural damage.

## 2. BP-Vehicle-Bridge Coupling for Bridge Structure Recognition

### 2.1 Bridge Structure Recognition Based on BPNN

In identifying structural damage in bridges, it is necessary to have a simple testing method for identification technology and memory ability. Thus, BPNN is suitable for identifying structural damage in bridges (Xiang et al., 2023; Xu et al., 2020). Identification and localization of the structural damage index is achieved using the BPNN's memory mechanism and capacity to forecast bridge dynamic characteristic parameters as output and structural damage as input. BPNN consists of three layers: input, output, and hidden. The model is shown schematically in Fig. 1.

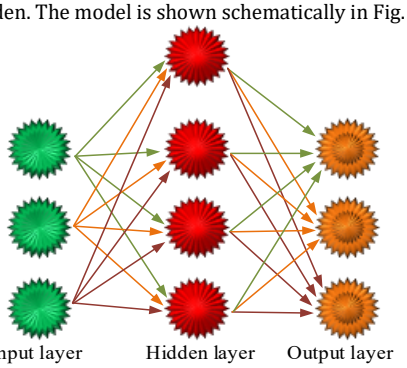


*Fig. 1 Schematic Diagram of BPNN Model*

In Fig. 1, the BPNN receives input signals, analyzes and processes the data in the hidden layer, and produces an output. The inputs to the nodes of the BPNN's hidden layer are calculated, as shown in Eq. (1).

$$x_j = \sum_i w_{ij} x_i \quad (1)$$

In Eq. (1), $x_j$ is each node of the hidden layer. $x_i$ is each node of the input layer. $w_{ij}$ is the connection weight between the input layer and each node of the hidden layer. The node output is calculated, as shown in Eq. (2).

$$y_j = \varphi(x_j) \quad (2)$$

In Eq. (2), $\varphi(x_j)$ is an activation function. The BPNN error can be described by an error function, as shown in Eq. (3).

$$E = \frac{1}{2}\sum_{j=1}^{M}(d_i - y_j)^2 \quad (3)$$

In Eq. (3), $M$ denotes the total number of neurons. The update network weights are calculated, as shown in Eq. (4).

$$\Delta W_{jk} = -\eta \frac{\partial E}{\partial W_{jk}} \quad (4)$$

In Eq. (4), "−" indicates a gradient descent, not positive or negative. When the BPNN model is run in reverse, each layer of the neural network inertia weights is rearranged between the output layers. Then, the computation is performed. After this repeated adjustment and calculation method, the neural network inertia weights are also continuously adjusted and updated until the output meets the error requirements, thus completing the calculation of the BPNN model. The process is shown on Fig.2.

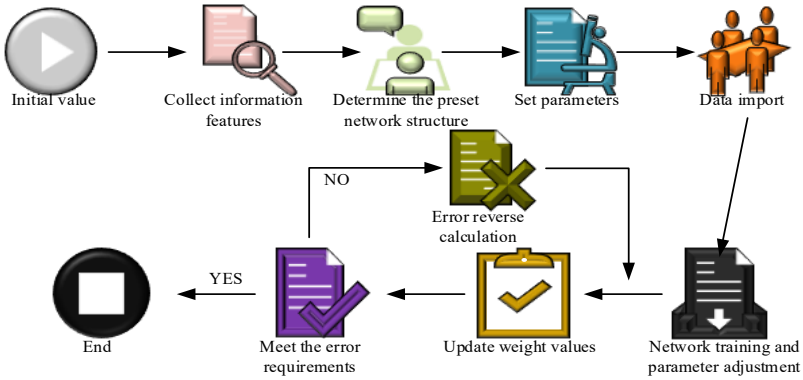


*Fig. 2 BPNN Operation Process*

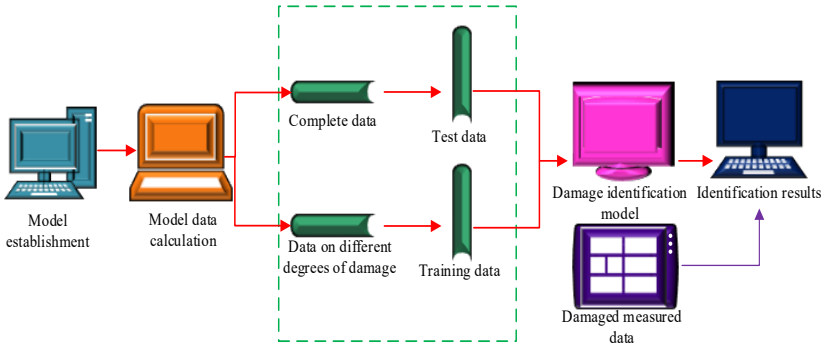


*Fig. 3 Damage Identification Process*

In Fig. 2, BPNN extracts information features. Then, the training data is imported and adjusted to numerically update the network weights. The BPNN is also completed when the error meets the requirements. When the error cannot meet the requirements, the error is reversed, and the weights are updated again until the error requirements are met. The deflection of the bridge structure must be controlled within a specific range in order to prevent stiffness from being too low. If the deflection is too great, the stiffness of the bridge structure will be diminished. Structural damage to the bridge leads to a reduction in stiffness. This results in an increase in the displacement change of the unit node due to the dynamic load through the bridge structure at the nodes of the unit node. Therefore, the displacement change of the unit node can express the bridge structure's damaged state. The unit node displacement is expressed in Eq. (5).

$$\{\Delta\} = [K]^{-1}\{P\} \tag{5}$$

In Eq. (5), $\{\Delta\}$ represents the unit node displacement vector of the bridge structure, $[K]$ represents the stiffness matrix of the bridge structure, and $\{P\}$ represents the unit node load vector. When the unit node load vector remains constant, the displacement vector of the bridge structure changes according to the stiffness matrix of the structure. In other words, the load vector of the bridge structure can represent its stiffness. A damaged recognition index based on the displacement change rate of the upper chord bar is established and expressed as Eq. (6).

$$\Delta x_i = \frac{x i_{imax}}{x_i} \tag{6}$$

In Eq. (6), $x_i$ represents the displacement at node $i$ when the stiffness of the bridge structure is perfect under the uncertain working conditions. $x_{imax}$ represents the maximum displacement at node $i$ when the stiffness of the bridge structure is imperfect and changed under the determined working conditions. $\Delta x_i$ represents the rate of change of the displacement at node $i$ when there is a load under the working conditions. The BPNN steps for recognizing bridge structure damage are shown in Fig. 3.

Fig.3 shows the process of damage identification using BPNN. First, a bridge finite element model is established, and the model data is calculated. Next, the damage location data are integrated, and the damage identification model is established. Then, the measured damage location data are simulated. Finally, the damage identification results are obtained. In the BPNN, the maximum value of the network output is used to judge the location and severity of damage to the chord bar. If the result is positive, the identification is correct. The specific expression is shown in Eq. (7).

$$0.8y \le \bar{y} \le 1.2y \tag{7}$$

In Eq. (7) $\bar{y}$ and $y$ are denoted as the actual output of the neural network and the single target output of the neural network, respectively.

## 2.2 Damage Identification Based on Coupled Axle Vibration Modeling

After using BPNN for bridge damage structure analysis, the secondary analysis of damage structure using axle coupled vibration can improve the accuracy of damage structure identification. In the process of a car passing through a bridge, the bridge will produce mutual vibration effect with the car. A vehicle-axle coupled vibration system is formed between the two (Zhang et al., 2021). The basic Eq. of vehicle-bridge coupling is described, as shown in Eq. (8).

$$F_b = M_b\ddot{y}_b + C_b\dot{y}_b + K_b y_b \tag{8}$$

In Eq. (8), $M_b$ denotes the bridge weight. $C_b$ denotes the bridge damping ratio. $K_b$ denotes the bridge stiffness matrix. $\ddot{y}_b$ denotes the single-target node acceleration. $\dot{y}_b$ denotes the single-target node velocity. $y_b$ denotes the single-target node displacement. $F_b$ denotes the kinetic load of the vehicle action over the bridge. Transforming the vehicle into a two-dimensional system, the vehicle-bridge model is shown in Fig. 4.

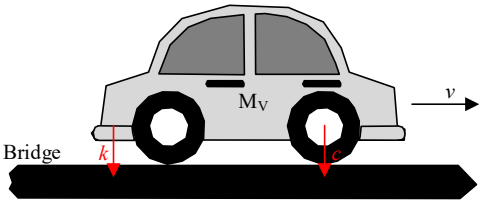


***Fig. 4 Vehicle-Bridge Model***

In Fig. 4, Mv is denoted as the mass of the vehicle. c and k denote the vertical downward stiffness and damping ratio of the vehicle passing over the bridge, respectively. The degrees of freedom of the wheels are not set in the vehicle-bridge model. Rather, the wheels act as a displacement link between the vehicle and the bridge deck. This relationship is expressed in Eq. (9).

$$Z_{wijl} = Z_b(x_{ijl}) + Z_S(x_{ijl}) \tag{9}$$

In Eq. (9), $x_{ijl}$ is expressed as the relative position of the $l$ th steering tire on the $j$ th steering wheel carrier of the $i$ th vehicle with respect to the bridge. According to the vehicle displacement conditions, the wheels and bridge deck always come into contact when a vehicle passes over the bridge. The relative displacement between the wheels and bridge deck can be described by Eq. (10).

$$z_i(x) = z_{vi}(x) - z_{bi}(x) - r_i(x) \tag{10}$$

In Eq. (10), $z_{vi}(x)$ represents the radial movement of the wheels through the bridge deck and $z_{bi}(x)$ represents the original radial displacement of the vehicle through the bridge deck. Due to the limitation of force balance, the force generated by the wheel for the bridge deck and the reaction force of the bridge deck to support the wheel remain the same and in the opposite direction. The expression relationship is shown in Eq. (11).

$$F_{vi} = -F_{bi} \tag{11}$$

In Eq. (11), $F_{bi}$ represents the force of the wheel on the bridge. Vehicle-bridge coupling system power equations can be solved in a number of methods. The study chooses to use the entire iterative approach for the calculation in order to obtain a quick and efficient iterative calculation of the vehicle-bridge coupling. The specific process is shown in Fig. 5.

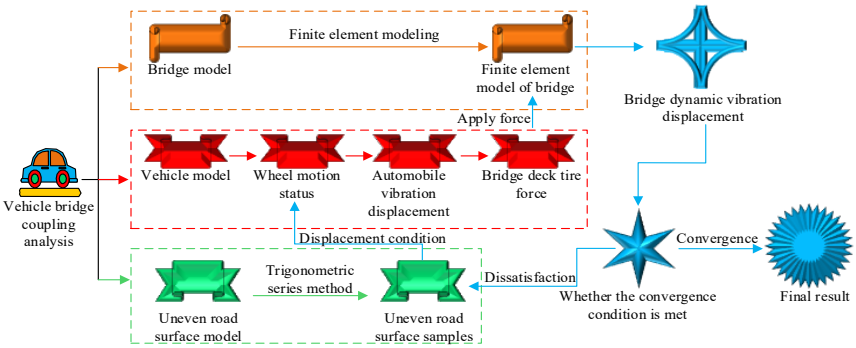


***Fig. 5 Vehicle-Bridge Coupling Calculation Process***

***Table 1. Classification of Road Surface Roughness Levels***

| Road surface grade | Road roughness coefficient $G_q(n_0) \times 10^{-6}\frac{m^2}{m^{-1}}n_0 = 0.1m^{-1}$ | | |
|---|---|---|---|
| | Lower limit | Geometric mean | Upper limit |
| A | 8 | 16 | 32 |
| B | 32 | 64 | 128 |
| C | 128 | 256 | 512 |
| D | 512 | 1024 | 2048 |
| E | 2048 | 4096 | 8192 |
| F | 8192 | 16384 | 32768 |
| G | 32768 | 65536 | 131072 |
| H | 131072 | 262144 | 524288 |

Fig. 5 shows the coupled vibration of the vehicle and bridge. This is obtained by establishing three models: pavement, vehicle, and bridge. The pavement samples and the motion state of the vehicle wheels are collected. Then, the interaction force between the pavement and the wheels is calculated iteratively. After establishing the bridge finite element model, the time course of vibration of the damaged bridge structure is converged. The final results are also obtained if the convergence condition is satisfied. If the convergence condition is not satisfied, the pavement samples are re-selected, and the operation is repeated until the convergence condition is satisfied. The axle coupling calculations are performed by coordinating the displacements and equilibrium forces. The convergence expression for displacement is shown in Eq. (12).

$$\frac{|Z_i^j - Z_i^{j-1}|}{Z_i^j} \le \varepsilon \tag{12}$$

In Eq. (12), $Z_i^j$ it denotes the displacement of the wheel from the bridge deck at the $j$th iteration. $Z_i^{j-1}$ denotes the displacement of the wheel from the bridge deck at the $j-1$th iteration. denotes the control parameter for convergence. The force convergence is expressed in Eq. (13).

$$\frac{|F_i^j - F_i^{j-1}|}{F_i^j} \le \varepsilon \tag{13}$$

In Eq. (13), $F_i^j$ represents the force acting on the bridge deck of the car tire in the $j$th iteration and $F_i^{j-1}$ represents the force acting on the bridge deck of the car tire in the $j-1$th iteration. In the actual vehicle-bridge coupling calculation, due to the unevenness of the road surface, which leads to the vibration of the car traveling on the bridge deck. The unevenness of the road surface is modeled. The density of road surface unevenness is expressed as Eq. (14).

$$G_d(n) = G_d(n_0)\left(\frac{n}{n_0}\right)^{-w} \tag{14}$$

In Eq. (14) $n$ and $n_0$ denote the frequency and reference frequency in the bridge deck in space, respectively. $\boldsymbol{G_d(n)}$ denotes the displacement rate Pu density. $G_d(n_0)$ denotes the bridge deck unevenness coefficient. The pavement unevenness classifications are shown in Table 1.

The unevenness of pavements can be viewed as a stable Gaussian equation that can be described using the triangular series method, the Fourier inverse transformation method, or the free regression moving average model method (Li et al., 2023). The power spectral densities of the bridge deck and pavement are used to model the methods used to change the pavement unevenness. For the calculation of pavement unevenness, the commonly used counting methods are the trigonometric series method and the power spectral density function, as shown in Eq. (15).

$$\begin{cases} r(x) = \sum_{i=1}^{n} G(n_1)\, cos(2\pi n_i x + \varphi_i) \\ G(n_i)^2 = 4G_d(n_i)\Delta n \end{cases} \tag{15}$$

In Eq. (15), $\varphi_i$ is a random number with values ranging from. $[0,2\pi]$. $G(n_i)$ is expressed as the magnitude of the vibration amplitude of the car crossing the bridge.

# 3. Validation of the Effectiveness of BPNN with Vehicle-Bridge Coupling Damage Identification

## 3.1 Effectiveness Analysis of Bridge Structure Damage Identification Using BPNN

A finite element model is created using a bridge on a high mountain pass as an example. The bridge's main beam is 60 meters long, and its main structure is made of concrete. The model consists of 58,135 units and 109,915 nodes. The BPNN model has a single hidden layer with 50 nodes. The number of nodes in the input layer is determined based on the number of dynamic characteristic parameters of the bridge. The number of nodes in the output layer is consistent with the requirements for identifying the location and extent of damage. The hidden layer uses the Sigmoid function, and the output layer uses a linear activation function. The iteration count is set to 1000, the learning rate is set to 0.01, and the Adam algorithm is used to accelerate convergence. The study sets the bridge structure as single damage under three different working conditions with stiffness reduction coefficients of 30%, 50%, and 70%, respectively. Five different noise degree conditions with noise sizes range from 0% to 20%, with an interval of 5%. The primary goal of identifying damage to a bridge structure is to locate the damaged structure and analyze the extent of the damage. The study uses a deep belief network (DBN) and a support vector machine (SVM) for comparison. The DBN's 3-layer restricted Boltzmann machine has 200, 100, and 50 nodes, a learning rate of 0.001, and a batch size of 32. The SVM's kernel function is Gaussian, and its regularization parameter is 1. The results are as Fig. 6.

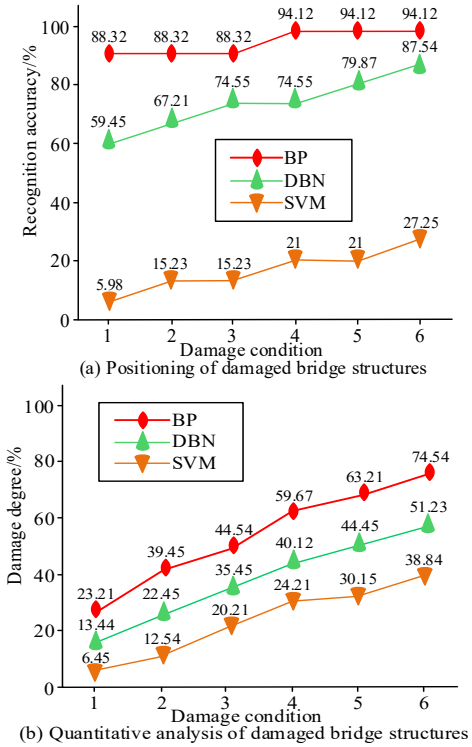


***Fig. 6 Identification, localization, and Quantitative Results of Three Methods under Different Operating Conditions***

As displayed in Fig. 6(a), the BPNN is smoother and has fewer extreme fluctuations in the process of locating the bridge structure than the other two methods when it comes to locating the damaged structure under various working conditions. Its minimum accuracy is 88.32%, and its maximum accuracy is 94.12%. The accuracy of DBN is 59.45% and 87.54% for the damaged structure. SVM has lower accuracy and a maximum of 27.25% when performing the localization of damaged bridges. In Fig. 6(b), the study suggested using BPNN for the quantitative analysis of structural damage with a higher accuracy than DBN and SVM methods, with the highest quantitative accuracy of 74.54%. The quantitative analysis of damage using BPNN is more accurate than the other two methods under various working conditions. The lowest quantitative accuracy using BPNN is 23.21%, which is about 10% higher than the other two methods. The lowest quantitative accuracy is 23.21%, about 10% higher than the other two methods. The results of damage localization and quantitative analysis of bridge structure under different noise levels are shown in Fig. 7.

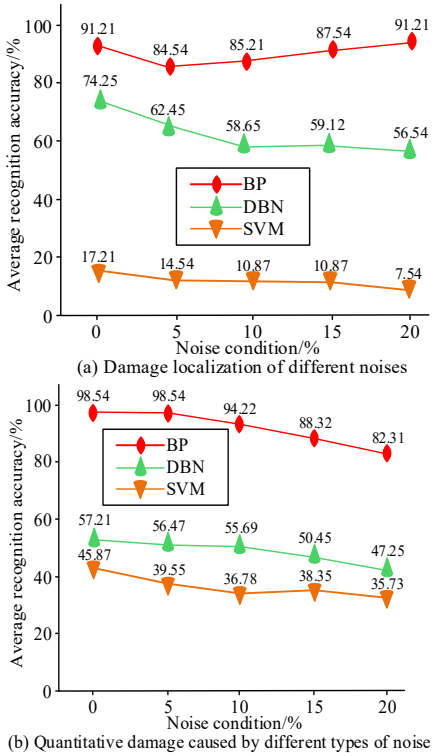


***Fig. 7 Damage Localization and Quantification under Different Noise Conditions***

In Fig. 7(a), the BPNN has a high localization accuracy for the damaged bridge structure under different noise conditions. It is less affected by the noise conditions, and the average accuracy of localization is 85%. Meanwhile, DBN and SVM are more affected by the noise and have a lower localization accuracy for the bridge structure. DBN achieves a localization accuracy of 74.25% at its highest and 56.54% at its lowest. The SVM algorithm has the highest localization accuracy, 17.21% and the lowest is 7.54%. The proposed BPNN model suggests that, as noise increases gradually, localization accuracy first decreases and then gradually recovers under noiseless conditions. This phenomenon may be related to the BPNN model's adaptive ability. When noise is low, the model begins to deviate from proper feature extraction and judgment, resulting in decreased localization accuracy. As noise levels increase, the BPNN model gradually learns to identify more discriminative and representative feature patterns in noisy data by continuously optimizing its weights and thresholds. This allows BPNN to more accurately identify damaged bridge features, resulting in improved localization accuracy. In Fig. 7(b), the quantitative accuracy of the BPNN model for the damaged bridge structure is high under conditions without noise influence, reaching 98.54%. With increasing noise, the quantitative accuracy gradually decreases, but the average accuracy remains at 90%. DBN has a quantitative accuracy of only 57.21% under noiseless conditions. Under the influence of increasing noise, the accuracy gradually decreases to 47.25%. SVM's accuracy is only 45.87% under noiseless conditions. The results of the three different algorithms for bridge structure multi-damage identification accuracy are shown in Fig. 8.

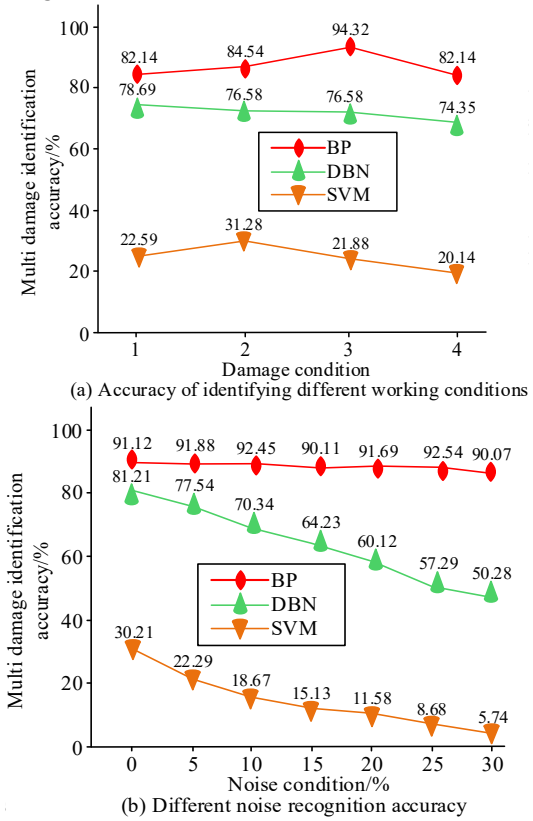


***Fig. 8 Identification Results of Multiple Structural Damages***

In Fig. 8(a), the BPNN has high accuracy in recognizing damage to the bridge structure under different working conditions. The highest accuracy reaches 94.32%, and the lowest accuracy is 82.14%. Compared with the DBN algorithm, the BPNN's accuracy is higher by about 5%. The SVM algorithm in different working conditions, for the bridge structure with multiple damage recognition accuracy is low, the highest accuracy of only 31.28%. The SVM algorithm has a lower accuracy in recognizing multiple damages of bridge structures under different working conditions, with a maximum accuracy of 31.28%. In Fig. 8(b), the BPNN maintains high accuracy in recognizing multiple types of damage to bridge structures under different levels of noise. In contrast, the recognition accuracy of the DBN and SVM algorithms decreases with increasing noise levels. Under the influence of 30% noise, the accuracy of DBN and SVM decreases to less than 50%, and the accuracy of BPNN remains above 90% under the influence of 30% noise. The accuracy of BPNN under the influence of 30% noise is still maintained at more than 90%. This demonstrates that the BPNN can accurately recognize multiple types of damage to a bridge structure under different working conditions and degrees of noise.

## 3.2 Validation of the Effectiveness of Secondary Damage Identification Using Vehicle-Bridge Coupling

After identifying and localizing the bridge damage structure using the BPNN, the bridge is subjected to varying degrees of damage for secondary identification to improve detection accuracy. This is achieved by analyzing various vehicle-bridge coupling parameters. The study uses vehicles traveling across three damaged bridge decks with respective damage coefficients of 0.1, 0.5, and 0.9 to examine the application of the vehicle-bridge coupling recognition model in conjunction with the BPNN. Fig. 9 shows the vehicle displacements taking place at various spans of the damaged bridge deck structure.

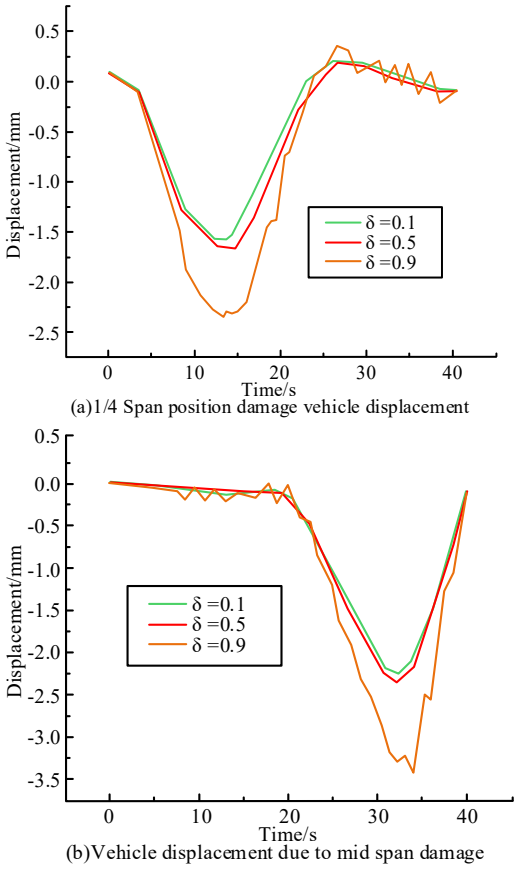


***Fig. 9 Vehicle Displacement with Different Span Damages***

In Fig. 9(a), when the damage degree of the bridge is 0.1, the displacement of the vehicle over the bridge increases gradually at the beginning. When it reaches 15 s, the displacement decreases gradually. At the 25th s, the displacement begins to be biased towards 0 mm. When the damage degree of the bridge is 0.5, the fluctuation of the displacement curve of the vehicle over the bridge becomes larger. At the 30th s, the displacement is biased towards 0 mm. When the bridge is 0.9, the vehicle starts to produce a large displacement at the beginning and is still being displaced at the cut-off time of the experiment. The vehicle displacement across the bridge begins to be large at the very beginning and is still occurring at the end of the experimental time. In Fig. 9(b), in the middle of the bridge span, when the damage degree of the bridge structure is 0.1, the displacement curve of the vehicle starting to drive over the bridge tends to be 0mm. When the time reaches about 20s, the displacement starts to be generated. When the damage degree of the bridge is 0.5, the displacement starts to occur when the vehicle drives over the bridge in about 10s. When it reaches its 20s, the displacement of the vehicle starts to intensify. When the damage level of the bridge structure is 0.9, the displacement of the vehicle starts when it crosses the bridge. Moreover, the displacement is still occurring until the end of the experiment. The above results show that when the bridge structure is damaged to a lower degree, the bridge damage location cannot be recognized by the vehicle displacement. However, when the bridge structure is damaged to a higher degree, the bridge damage location can be recognized by the displacement generated by the vehicle driving over the bridge deck. Fig. 10 shows the wavelet coefficients of vehicles at different span locations.

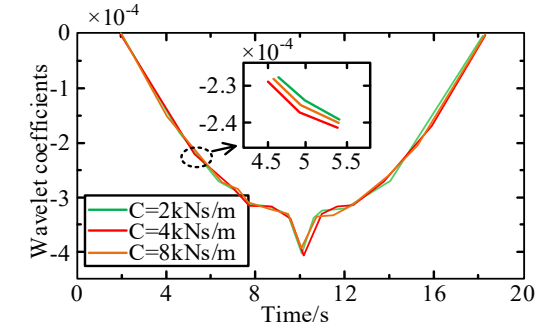


(a)Wavelet coefficients of different damping of vehicles

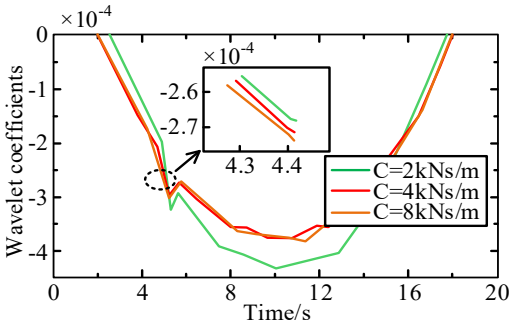


(b)Wavelet coefficients of different damping for 1/4 vehicle

***Fig. 10 Different Damping Wavelet Coefficients of Vehicles at Different Span Positions***

As displayed in Fig. 10(a), when the span position is full, the wavelet coefficients of the various vehicle damping nearly overlap and do not differ significantly. This has a negative impact on identifying the bridge's damaged structure, and there are fluctuations in the damaged areas of the structure. However, the trend of the wavelet coefficients of the three types of damping curves tends to be similar, which makes locating the damaged structure more difficult. In Fig. 10(b), when the span position becomes 1/4, the wavelet coefficients of different damping of the vehicle overlap less. Moreover, there are more obvious fluctuations of wavelet coefficients in the damaged parts of the bridge structure, which can recognize the damaged structure of the bridge with higher accuracy. The above results show that for the vehicle-bridge coupling, different damping of vehicles has an effect on the identification and localization of the damaged bridge structure. Furthermore, the different damping of vehicles in the 1/4 span position has a higher accuracy for the identification of the damaged bridge structure. The wavelet coefficients of different speeds of vehicles in different span positions are as Fig. 11.

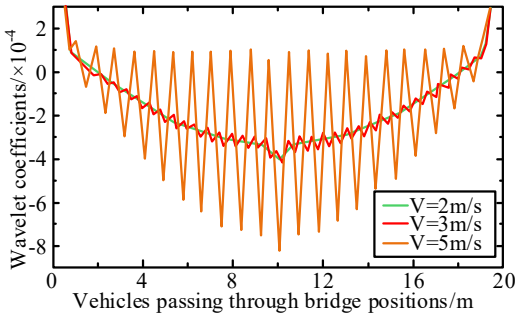


(a)Wavelet coefficients at different speeds at mid span positions

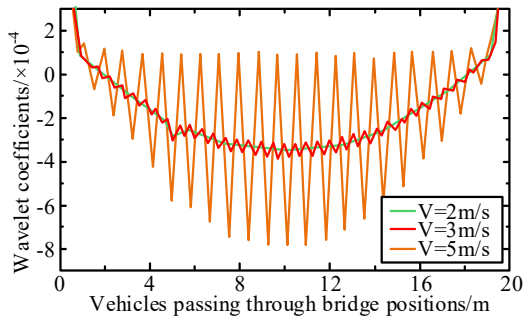


(b)Wavelet coefficients of different velocities at 1/4 mid span position

***Fig. 11 Wavelet Coefficients of Vehicles at Different Speeds in Different Span Positions***

In Fig. 11(a), when the vehicle is in the middle of the bridge and traveling at 2 m/s, the wavelet coefficient change curve is smoother and less fluctuating. This improves the ability to recognize the damaged local structure of the bridge. The loss position of the bridge can be calculated using the vehicle-bridge coupling equation. When the vehicle speed is kept at 3m/s, the fluctuation of wavelet coefficient change curve is more obvious. At this time, the vibration of the vehicle driving over the bridge can be observed to a larger extent. When the vehicle speed is kept at 5m/s, the wavelet coefficient change curve fluctuates violently. At this time, the wavelet coefficient fluctuation has obscured the fluctuation caused by the damaged structure of the bridge, resulting in the inability to accurately identify the location of the damaged structure of the bridge. In Fig. 11(b), it is obvious that in the position of 1/4 span of the bridge deck, which is consistent with Fig. 11(a), the vehicle-bridge coupling calculations can be carried out at a lower speed to recognize the location and degree of the damaged structure of the bridge at a lower level. When the speed is too high, the fluctuation change curve is violent, and the vehicle-bridge coupling calculation cannot be carried out at a higher level. It is obvious that when the bridge damaged structure is recognized by vehicle-bridge coupling, the bridge structural damage can be recognized better when the speed is lower, but not better when the speed is higher. To verify the practical application of the proposed method, the effect is tested on a bridge with three types of damage. High-precision sensors are used to collect vibration response data of the bridge under different working conditions. The collected data is then preprocessed with filtering and noise reduction. The preprocessed data is divided into training and testing sets at a ratio of 7:3. Then, compare the accuracy and recall of the proposed method with those of traditional BPNN, Faster RCNN, and YOLOv5s. The results are shown in Table 2.

***Table 2. Comparison of Accuracy and Recall of Four Methods***

| Method | Accuracy/% | Recall/% |
|---|---|---|
| BPNN | 88.75 | 86.49 |
| Faster RCNN | 91.34 | 88.98 |
| YOLOv5s | 90.13 | 88.37 |
| Proposed method | 95.62 | 94.91 |

In Table 2, the proposed method has the highest accuracy and recall, at 95.62% and 94.91%, respectively. These values are 6.87% and 8.42% higher than those of traditional BPNN.

## 4. Conclusion

The study proposes a method of identifying and localizing bridge structural damage using BPNNs and axle interaction to address the problem of continuous detection and maintenance of bridge damage. The findings demonstrated that BPNN has high recognition accuracy for localizing damaged structures under various working conditions. The lowest accuracy was 88.32%, and the highest was 94.12%. Additionally, the identification process is faster and more seamless, with recognition accuracy roughly 10% higher than that of the DBN and SVM algorithms. The BPNN is less affected by noise and can achieve over 85% localization accuracy even when there is varying degrees of noise interference. In contrast, the DBN and SVM algorithms are more affected by noise and can only achieve an average accuracy of about 50% in recognizing the degree of damage to the bridge structure. In the identification of damaged bridge structure through vehicle-bridge coupling, it can better identify and localize the damage degree of bridge structure through displacement. When the damping is different, the wavelet coefficient change of the damping can be used to accurately recognize the location of the bridge damage structure and the degree of damage when the vehicle drives over the bridge. When crossing the bridge, the vehicle's speed is kept below 3 m/s, causing its wavelet coefficient curve to fluctuate significantly. The time at which the change occurs can be used to pinpoint the location of bridge damage, with recognition accuracy as high as 80%. In summary, the suggested approach can precisely pinpoint the location and extent of structural deterioration of a bridge, but only when identifying structural damage caused by vehicles driving over the bridge deck. Future repairs will consider the location and multi-structural damage caused by vehicles moving across the bridge deck.

## Reference

Chen, D., Cui, H., Li, Z., Xu, S., & Zhang, Y. (2024). Indirect identification and analysis of bridge damage using vehicle-bridge coupled vibration and deep learning. Journal of Performance of Constructed Facilities, 38(4), 4016-4028. https://doi.org/10.1061/JPCFEV.CFENG-472

Chen, D., Zhang, Y., Wan, R., Li, Z., Xu, S., & Yang C. (2024). Indirect identification of bridge damage based on coupled vehicle-bridge vibration and 2D-CNN. Measurement Science and Technology, 35(5), 19-31. https://doi.org/10.1088/1361-6501/ad2ad5

Corbally, R., & Malekjafarian, A. (2021). Examining changes in bridge frequency due to damage using the contact-point response of a passing vehicle. Journal of Structural Integrity and Maintenance, 6(3), 148-158. https://doi.org/10.1080/24705314.2021.1906088

Hao, H., Wei, W., & Lei, H. (2020). Intelligent recognition of bridge damage based on convolutional neural network and recursive graph. Chinese Journal of Applied Sciences, 28(4), 966-980. https://doi.org/10.16058/j.issn.1005-0930.2020.04.018

He, H., Zheng, J., Liao, L., & Chen, Y. (2021). Damage identification based on convolutional neural network and recurrence graph for beam bridge. Structural Health Monitoring, 20(4), 1392-1408. https://doi.org/10.1177/1475921720916928

Li, Z., Xiang, C., Qi, X., & Yang, H. (2023). Numerical analysis of continuous beam bridge damage identification based on vehicle response. Earthquake Engineering and Engineering Vibration, 43(2), 202-211. https://doi.org/10.13197/j.eeed.2023.0220

Malekjafarian, A., Golpayegani, F., Moloney, C., & Clarke, S. (2019). A machine learning approach to bridge-damage detection using responses measured on a passing vehicle. Sensors, 19(18), 4035-4053. https://doi.org/10.3390/s19184035

Neves, A. C., González, I., Karoumi, R., & Leander, J. (2021). The influence of frequency content on the performance of artificial neural network–based damage detection systems tested on numerical and experimental bridge data. Structural Health Monitoring, 20(3), 1331-1347. https://doi.org/10.1177/1475921720924320

Nguyen, D. H., Bui, T. T., De Roeck, G., & Wahab, M. A. (2019). Damage detection in Ca-Non-Bridge using transmissibility and artificial neural networks. Structural Engineering and Mechanics, 71(2), 175-183. https://doi.org/10.12989/sem.2019.71.2.175

Nick, H., & Aziminejad, A. (2021). Vibration-based damage identification in steel girder bridges using artificial neural network under noisy conditions. Journal of Nondestructive Evaluation, 40(1), 15-43. https://doi.org/10.1007/s10921-020-00744-8

Sony, S., Gamage, S., Sadhu, A., & Samarabandu, J. (2022). Multiclass damage identification in a full-scale bridge using optimally tuned one-dimensional convolutional neural network. Journal of Computing in Civil Engineering, 36(2), 35-49. https://doi.org/10.1061/(ASCE)CP.1943-5487.0001003

Wu, R., & Zhang, C. (2023). Analysis of bridge vibration response for identification of bridge damage using BP neural network. Nonlinear Engineering, 12(1), 273-281. https://doi.org/10.1515/nleng-2022-0273

Xiang, C., Shi, H., & Yang, R. (2023). Research on bridge damage identification method based on modal frequency strain energy entropy and tent SSA BP neural network. Highway, 68(3), 143-150.

Xu, C., Yu, Q., & Yang, Q. (2020). Structural damage identification technology based on BP neural network. Applied Technology, 47(3), 63-68. https://doi.org/10.11991/yykj.202004001

Yessoufou, F., & Zhu, J. (2023). Classification and regression-based convolutional neural network and long short-term memory configuration for bridge damage identification using long-term monitoring vibration data. Structural Health Monitoring, 22(6), 4027-4054. https://doi.org/10.1177/14759217231161811

Zhang, H., Zhong, Z., Duan, J., Yang, J., Zheng, Z., & Liu, G. (2022). Damage identification method for medium-and small-span bridges based on macro-strain data under vehicle-bridge coupling. Materials, 15(3), 1097-1113. https://doi.org/10.3390/ma15031097

Zhang, Y., Ma, C., & Chen, P. (2021). Bridge structural damage identification based on vehicle bridge coupling vibration. Highway Engineering, 46(2), 60-6470. https://doi.org/10.19782/j.cnki.1674-0610.2021.02.010

Zhao, L. (2024). Prediction of vibration response of simply supported beam bridge structure based on BP artificial neural network. Journal of Shenyang University of Technology, 46(3), 347-352. https://doi.org/10.7688/j.issn.1000-1646.2024.03.16

Zhi, Z., Xue, L., & Cheng, W. (2023). Research on single damage identification of continuous beam bridges with equal cross-section based on vehicle bridge coupling. Journal of Hefei University of Technology: Natural Science Edition, 46(6), 813-821.

Zong, S., & Yi, C. (2020). Online speed and weight recognition based on cable force monitoring of cable-stayed bridges. Vibration and Shock, 39(17), 134-141. https://doi.org/10.13465/j.cnki.jvs.2020.17.018

## Disclaimer